Random-phase-approximation ground-state correlations and the isotope effect in the ^{40}Ca and ^{48}Ca

E. Tinková
Nuclear Research Institute, ČSKAE, CS 250 68 Řež, Czechoslovakia

M. Gmitro
Institute of Nuclear Physics, Czechoslovak Academy of Sciences, CS 250 68 Řež, Czechoslovakia

(Received 12 November 1975; revised manuscript received 14 April 1976)

Ellis's method of constructing the random-phase-approximation ground-state wave function which avoids the earlier dubious and incorrect quasiboson approximation is extended to the $N \neq Z$ nuclei. The most important effects arise from the appropriate treatment of the isospin quantum number. In application to the calcium isotopes we find that the calculated relative shift of the proton rms radius from ^{40}Ca to ^{48}Ca $R = -0.35\%$ for the first time agrees with the high energy electron scattering result $R = -0.31\%$. Excellent agreement is also obtained for the difference of the neutron and proton rms radii in ^{48}Ca. It should be emphasized, however, that our conclusions concerning the magnitude of the effects on the rms radii due to ground state correlations are more significant than the detailed comparison with experiment.

[NUCLEAR STRUCTURE ^{40,48}Ca; calculated spectra, shell breaking, rms radii, and density distributions. Ground-state correlations and isospin projection.]

I. INTRODUCTION

The original shell-model assumptions relying on the picture of the closed shells of the magic nuclei are clearly qualitative only. Extensive experimental observations and theoretical investigations have shown that appreciable core excitation components are present in the ground state (g.s.) wave function of the magic nuclei. The nuclear random-phase approximation (RPA)[1] provides the necessary theoretical framework for the investigation of such correlations. As early as 1963 Brown and Jacob,[2] using a schematic interaction, obtained an explicit form of the RPA ground-state wave function. Sanderson[3] and Agassi, Gillet and Lumbroso[3] then investigated several examples of doubly magic nuclei with a residual force of finite range. They found a considerable depletion of the closed-shell component of the ground state ranging from 40 to 80%. A common error of the early investigators[3] consisted in the double counting of certain RPA graphs.[4] Performing the explicit summation of the needed diagrams, Ellis[4] obtained the correct RPA ground-state wave function. Within this new formalism the correlations are strongly reduced but are still appreciable and even large for particular nuclei.

The problem of the ground-state correlations is slightly more complicated in the case of the magic nuclei with $N \neq Z$ if a sharp value $T_0 = \frac{1}{2}(N-Z)$ of the isospin is required. Namely, after a particle-hole (p-h) pair is excited the resulting isospin T of the configuration is formed by vector coupling of the core isospin T_0 and that of the p-h pair T_{ph}. With $T_0 \neq 0$, two possibilities are open when $T_{\text{ph}} = 1$: $T = T_0$, $T_0 + 1$. Separation of these two components must be ensured in the formalism, because the nuclear interaction conserves isospin and the long-range Coulomb force causes very little mixing inside the nucleus: Isospin seems to be a meaningful quantum number.[5] The existence of isobaric analog states provides a most striking demonstration of it. Some problems of the g.s. and analog states in $N \neq Z$ nuclei have been studied within the Hartree-Fock approximation. E.g., Engelbrecht and Lemmer[5] and Lee[5] have discussed the cases where the isospin symmetry of the Hartree-Fock (HF) wave functions is restored in $N \neq Z$ nuclei after introduction of the RPA-type neutron-proton correlations.

Following our previous calculation[6] we extend the RPA ground-state theory to the $N \neq Z$ nuclei by improving the basis states with respect to the isospin. An attempt in this direction has been made by Parikh.[7] We present here a new and more transparent formulation and perform detailed numerical calculations which are practically absent in Ref. 7.

The new formalism was developed with the aim of studying in detail the well known anomaly experimentally observed[8] in the root-mean-square radii of the calcium isotopes: They do not follow the usual $A^{1/3}$ rule. Our methods are suitable for the description of the ^{40}Ca and ^{48}Ca nuclear ground states and we show in a numerical calculation that the g.s. correlations are important and provide an adequate explanation of the anomaly.

The paper is planned as follows: The isospin projected ground-state wave function of the $N \neq Z$ nuclei is constructed in Sec. II. The excitation spectra, obtained as a byproduct in our calculation, ground-state decompositions, the results for the root-mean-square radii, and the density distributions are given in Sec. III. Finally, Sec. IV contains the conclusions.

II. RPA GROUND-STATE WAVE FUNCTION WITH DEFINITE ISOSPIN

A. Isospin operators

In $N \neq Z$ magic nuclei the vacuum $|T_0 T_0\rangle$ is assumed to have no correlations built into it. The total isospin operators are defined as in Ref. 9:

$$T^{+} = \sum_{jm} b^{\dagger}_{jm} a_{jm} ,$$
$$T^{-} = \sum_{jm} a^{\dagger}_{jm} b_{jm} , \qquad (1)$$
$$T^{0} = \frac{1}{2} \sum_{jm} (b^{\dagger}_{jm} b_{jm} - a^{\dagger}_{jm} a_{jm}) ,$$

where $a^{\dagger}_{jm}$ and $b^{\dagger}_{jm}$ are the creation operators for protons and neutrons, respectively. We list here also the commutation relation between the operators T^{+} and T^{-},

$$[T^{+}, T^{-}] = 2T^{0} , \qquad (2)$$

and the only nonvanishing commutators between the T^{+} and T^{-} operators and particle creation (annihilation) operators,

$$[T^{+}, a^{\dagger}_{jm}] = b^{\dagger}_{jm} , \quad [T^{+}, b_{jm}] = -a_{jm} ,$$
$$[T^{-}, b^{\dagger}_{jm}] = a^{\dagger}_{jm} , \quad [T^{-}, a_{jm}] = -b_{jm} . \qquad (3)$$

Then in our notation:

$$T^{+} |T_0 T_0\rangle = 0 ,$$
$$T^{0} |T_0 T_0\rangle = T_0 |T_0 T_0\rangle . \qquad (4)$$

B. Basis states

The orthonormal basis states with definite isospin are obtained in three steps.

(i) The operators

$$\Omega^{\dagger}_{P}(i, JM) = \sum_{m_{pi} m_{hi}} (-)^{j_{hi} - m_{hi}} \begin{bmatrix} j_{p_i} & j_{h_i} & J \\ m_{p_i} & -m_{h_i} & M \end{bmatrix} a^{\dagger}_{p_i m_{pi}} a_{h_i m_{hi}} ,$$

$$\Omega^{\dagger}_{N}(i, JM) = \sum_{m_{pi} m_{hi}} (-)^{j_{hi} - m_{hi}} \begin{bmatrix} j_{p_i} & j_{h_i} & J \\ m_{p_i} & -m_{h_i} & M \end{bmatrix} b^{\dagger}_{p_i m_i} b_{h_i m_{hi}} , \qquad (5)$$

which, acting on the uncorrelated shell-model ground state $|T_0 T_0\rangle$, create the 1p-1h proton and neutron states

$$|\alpha_i\rangle = \Omega^{\dagger}_{P(N)}(i, JM) |T_0 T_0\rangle$$

are introduced. Here the symbol $[\because]$ denotes the Clebsch-Gordan coefficient. Though orthonormal, the sets $|\alpha_i\rangle$ contain isospin impurities.

(ii) Löwdin's[10] projection operators P_{TT_z} are used to obtain the states with definite isospin

$$|\beta_i\rangle = P_{TT_z} |\alpha_i\rangle .$$

The explicit form of P_{TT_z} can easily be written in terms of T^{-} and T^{+}:

$$P_{TT_z} = (2T+1) \frac{(T+T_z)!}{(T-T_z)!} \times \sum_{\nu=0}^{\nu_{\max}} (-)^{\nu} \frac{(T^{-})^{T-T_z+\nu} (T^{+})^{T+T_z+\nu}}{\nu!(2T+\nu+1)!} , \qquad (6)$$

where $\nu_{\max}$ is finite and specified in Ref. 10. In particular, when acting on $\Omega^{\dagger} |T_0 T_0\rangle$ the projector is, e.g., $P_{T_0 T_0} = 1 - \frac{1}{2} T^{-} T^{+} / (T_0 + 1)$. In general, the projected states are not orthonormal and may form an overcomplete set.

(iii) The unitary matrix S which diagonalizes the metric matrix N whose elements are

$$N_{kl} = \langle \beta_k | \beta_l \rangle$$

provides us also[11] with the desired orthonormal set

$$|\gamma_i\rangle = \frac{1}{\sqrt{\lambda_i}} \sum_{j} S_{ij} |\beta_j\rangle ,$$

λ_i being the eigenvalues of the matrix N. Naturally, if the set $|\beta_i\rangle$ was overcomplete, one or several zero eigenvalues λ appear. The corresponding eigenvectors should be omitted in construction of the set $|\gamma_i\rangle$.

Let us note that this construction remains unchanged if the operators (5) have a more complicated (e.g., m-particle–n-hole) structure. In the case of 1p-1h configuration the result is actually very simple.

We denote by f the single-particle levels in the neutron excess region. The set $|\gamma_i\rangle$ is constructed from $|T_0 T_0\rangle$ by the operators

$$\Gamma^{\dagger}_{TT_z}(i, JM) = P_{TT_z} A^{\dagger}(i, JM) , \qquad (7)$$

where $A^{\dagger} = \Omega^{\dagger}_{P}$ ($A^{\dagger} = \Omega^{\dagger}_{N}$) of Eq. (5) if $p_i = f$ ($h_i = f$). In the case of both $p_i \neq f$ and $h_i \neq f$ we have

$$A^{\dagger}(i, JM) = \frac{1}{\sqrt{2}} [\Omega^{\dagger}_{P}(i, JM) + \Omega^{\dagger}_{N}(i, JM)] \qquad (8a)$$

and

$$A^\dagger(i+1,JM)=\frac{1}{\sqrt{2}}[\Omega_P^\dagger(i,JM)-\Omega_N^\dagger(i,JM)]\,. \qquad (8b)$$

It is well known[9] that an additional 2p-2h admixture of the form $b^\dagger a T^-$ is generated in the last case, namely,

$$P_{T_0T_0}\frac{1}{\sqrt{2}}[\Omega_P^\dagger-\Omega_N^\dagger]\,|T_0T_0\rangle = \left(\frac{T_0}{2(T_0+1)}\right)^{1/2}\sum_{m_{pi}m_{hi}}(-)^{j_{hi}-m_{hi}}\begin{bmatrix} j_{p_i} & j_{h_i} & J\\ m_{p_i} & -m_{h_i} & M\end{bmatrix}\left(a^\dagger_{p_im_{pi}}a_{h_im_{hi}}-b^\dagger_{p_im_{pi}}b_{h_im_{hi}}-\frac{1}{T_0}b^\dagger_{p_im_{pi}}a_{h_im_{hi}}T^-\right)|T_0T_0\rangle\,. \qquad (9)$$

The linearized index i labels the independent operators $\Gamma^\dagger$. The final set $|\gamma_i\rangle$ happens to be identical with the choice of Jaffrin and Ripka.[12] It can be checked that the operators $\Gamma^\dagger_{T_0T_0}(i,JM)$ together with their Hermitian conjugate $\Gamma_{T_0T_0}(i,JM)$ satisfy the following relations required in the RPA formalism:

$$\Gamma_{T_0T_0}(i,JM)\,|T_0T_0\rangle=0\,, \qquad (10)$$

$$\langle T_0T_0|[\Gamma_{T_0T_0}(i,JM),\Gamma^\dagger_{T_0T_0}(j,JM)]\,|T_0T_0\rangle=\delta_{ij}\,. \qquad (11)$$

Commutation relations of the $\Gamma^\dagger_{T_0T_0}(i,JM)$ operators with particle (hole) number operators $\sum_{m_k}a^\dagger_{km_k}a_{km_k}$, $\sum_{m_k}b^\dagger_{km_k}b_{km_k}$ ($\sum_{m_r}a_{rm_r}a^\dagger_{rm_r}$, $\sum_{m_r}b_{rm_r}b^\dagger_{rm_r}$) will be needed in the forthcoming application. Their derivation is straightforward; we list here as an example the result for the neutron particle number operator

$$\sum_{m_k}[b^\dagger_{km_k}b_{km_k},\Gamma^\dagger_{T_0T_0}(j,JM)] = \delta_{kp_j}\sum_{m_{pj}m_{hj}}(-)^{j_{hj}-m_{hj}}\begin{bmatrix} j_{p_j} & j_{h_j} & J\\ m_{p_j} & -m_{h_j} & M\end{bmatrix}G^{(j)}\,, \qquad (12)$$

where $G^{(j)}=0$ if $p_j=f$ and $G^{(j)}=b^\dagger_{p_jm_{pj}}b_{h_jm_{hj}}$ if $h_j=f$. If both $p_j\neq f$ and $h_j\neq f$ then

$$G^{(j)}=\frac{1}{\sqrt{2}}\,b^\dagger_{p_jm_{pj}}b_{h_jm_{hj}}\,,$$

$$G^{(j+1)}=-\left(\frac{T_0}{2(T_0+1)}\right)^{1/2}\times\left(b^\dagger_{p_jm_{pj}}b_{h_jm_{hj}}+\frac{1}{T_0}b^\dagger_{p_jm_{pj}}a_{h_jm_{hj}}T^-\right).$$

C. RPA equations

We are looking for the operators $O_\lambda^\dagger$ which create nuclear excited states $|\lambda\rangle$ out of a parent state $|\Psi\rangle$:

$$O_\lambda^\dagger|\Psi\rangle=|\lambda\rangle\,,$$
$$O_\lambda|\Psi\rangle=0\,. \qquad (13)$$

To derive suitable equations for $O_\lambda^\dagger$ Rowe[13] started with formally exact equations of motions

$$\langle\Psi|[O_\kappa,[H,O_\lambda^\dagger]]|\Psi\rangle=\omega\langle\Psi|[O_\kappa,O_\lambda^\dagger]|\Psi\rangle\,. \qquad (14)$$

To proceed further, two main approximations are usual. First, the operators $O_\lambda^\dagger$ are sought in a strongly restricted space [see Eq. (19) for our choice]. Secondly, instead of the exact ground state $|\Psi\rangle$ an approximation $|\phi\rangle$ is chosen with the argument that Eq. (14) is, in fact, not very sensitive to $|\Psi\rangle$. Finally, this approximation can be improved by iterating Eq. (13).

We would like to stress that Eq. (14) relates the ground-state expectation values of certain operators rather than the operators themselves. In this formalism several earlier difficulties (e.g., uncertainty of the so-called linearization procedure) are avoided. Most important and unlike the other derivations, Eq. (14) is not limited to the Hartree-Fock form of the ground state.[13,14] Using this advantage of the double commutator equations we need not concern ourselves with the isospin properties of the HF states in $N\neq Z$ nuclei and can safely use the uncorrelated shell-model ground state $|T_0T_0\rangle$ in the capacity of $|\phi\rangle$ as a suitable approximation to $|\Psi\rangle$. Because of the arbitrariness of $|\phi\rangle$, Hermiticity of Eq. (14) may be lost. To reestablish it, Rowe[13] introduces the symmetrized double commutators

$$[A,H,B]=\tfrac{1}{2}([[A,H],B]+[A,[H,B]]) \qquad (15)$$

to obtain well-behaved equations of motion

$$\langle\phi\,|[O_\kappa,H,O_\lambda^\dagger]|\,\phi\rangle=\omega\langle\phi|[O_\kappa,O_\lambda^\dagger]\,|\phi\rangle \qquad (16)$$

which follow from Eq. (14) in the limit that $|\phi\rangle$ is an eigenstate of H, since then

$$\langle\phi\,|[[O_\kappa,O_\lambda^\dagger],H]\,|\phi\rangle=0\,. \qquad (17)$$

The uncoupled equations of motion (16) were frequently used to describe the $N=Z$ nuclei, where the standard vector coupling techniques help to construct the operators $O_\lambda^\dagger(JMTM_T)$. Since the ground-state total spin and isospin is $J_0 = T_0 = 0$ here, the excited states (13) are characterized by the sharp values of J and T.

For $N > Z$ the ground state, though scalar in the J space, has tensorial properties in the isospin space. Tensor equations of motion have been suggested by Rowe and Ngo Trong[14] to settle this problem without introducing additional complexities into the operators $O_\lambda^\dagger$. The price to be paid for this is a more complicated structure and a certain asymmetry of the resulting matrix equations. Indeed a ground state is assumed in Ref. 14 but no attempt was made there to derive it. The authors argue that the method of the tensor equations of motion being designed for the study of the nuclear excitation dynamics need not be equally well suited for the description of the static ground-state properties.

We are mainly interested in the ground-state characteristics of the $N > Z$ nuclei. The uncoupled form of the equations of motion (16) is therefore maintained. To separate the excited states with good isospin, the projection operators[10] P_{TT_z}, which we have already discussed, were used. Employing the relation $[H, P_{TT_z}] = 0$, Eq. (16) may readily be rewritten as

$$\langle T_0T_0|[Q_\kappa, H, Q_\lambda^\dagger]\,|\,T_0T_0\rangle = \omega\langle T_0T_0|[Q_\kappa, Q_\lambda^\dagger]\,|\,T_0T_0\rangle\,, \tag{18}$$

since $\langle T_0T_0|[[Q_\kappa, Q_\lambda^\dagger], H]|T_0T_0\rangle = 0$ as required. The symbol $Q_\lambda^\dagger$ is a shorthand notation for $Q_{TT_0}^\dagger(\lambda, JM)$ which we choose to be

$$Q_{TT_0}^\dagger(\lambda, JM) = \sum_i [X_i(\lambda)\Gamma_{TT_0}^\dagger(i, JM) + Y_i(\lambda)\Gamma_{TT_0}(i, J - M)]\,. \tag{19}$$

Then the expansion coefficients X_i and Y_i are the solutions of the matrix equations

$$\begin{pmatrix} A & B \\ -B & -A \end{pmatrix}\begin{pmatrix} X \\ Y \end{pmatrix} = \omega\begin{pmatrix} X \\ Y \end{pmatrix} \tag{20}$$

with submatrices defined as

$$A_{ij} = \langle T_0T_0|[\Gamma_{TT_0}(i, JM), H, \Gamma_{TT_0}^\dagger(j, JM)]\,|\,T_0T_0\rangle\,,$$

$$B_{ij} = \langle T_0T_0|[\Gamma_{TT_0}(i, JM), H, \Gamma_{TT_0}(j, J-M)]\,|\,T_0T_0\rangle\,. \tag{21}$$

The detailed structure of matrices A and B with $T = T_0$ is given in Table I. As for the 2p-2h admixtures of the state (9) consider, e.g., the term

$$\langle T_0T_0|\,T^+a^\dagger bHb^\dagger aT^-\,|T_0T_0\rangle \tag{22}$$

of the matrix A. Using the commutators (2) and (3) we can interchange the positions of T^+ and T^- in (22). In effect we obtain a linear combination of the usual 1p-1h matrix elements since $T^+|T_0T_0\rangle$

TABLE I. RPA matrix of the nuclear Hamiltonian. The different configurations are labeled by the operator $A^\dagger$ used in Eq. (7). Contributions E_i to matrix A from the single-particle Hamiltonian are given in the first entry, where $\epsilon_i = \frac{1}{2}(\epsilon_{p_i}^P - \epsilon_{h_i}^P + \epsilon_{p_i}^N - \epsilon_{h_i}^N)$, $\delta\epsilon_i = (\epsilon_{p_i}^P + \epsilon_{h_i}^P - \epsilon_{p_i}^N - \epsilon_{h_i}^N)/2T_0$. Note the nondiagonal term $E_i^{\text{off}} = \frac{1}{2}[(T_0+1)/T_0]^{1/2}(\epsilon_{p_i}^P - \epsilon_{h_i}^P - \epsilon_{p_i}^N + \epsilon_{h_i}^N)$. To obtain the interaction term of the matrices A and B insert $F_T = F(p_ih_ip_jh_jJT)$ and $F_T = -(-)^{j_{p_j}+j_{h_j}+J+T} \times F(p_ih_ih_jp_jJT)$, respectively, into the second entry, where $a = [2T_0/(T_0+1)]^{1/2}$. The "hole-particle coupled" matrix elements $F(abcdJT)$ are those of Ref. 6; ϵ_p^P, ϵ_h^P, ϵ_p^N, and ϵ_h^N denote the energies of the shell-model single-particle states for the proton particle, proton hole, neutron particle, and neutron hole, respectively.

Type of configuration	$\Omega_P^\dagger$	$\Omega_N^\dagger$	$2^{-1/2}[\Omega_P^\dagger + \Omega_N^\dagger]$	$2^{-1/2}[\Omega_P^\dagger - \Omega_N^\dagger]$
$\Omega_P^\dagger$	$E_i = \epsilon_{p_i}^P - \epsilon_{h_i}^P$			
	$-F_0 - F_1$	$-F_0 + F_1$	$-\sqrt{2}F_0$	$-aF_1$
$\Omega_N^\dagger$		$E_i = \epsilon_{pi}^N - \epsilon_{hi}^N$		
	$-F_0 + F_1$	$-F_0 - F_1$	$-\sqrt{2}F_0$	aF_1
$2^{-1/2}[\Omega_P^\dagger + \Omega_N]$			$E_i = \epsilon_i$	E_i^{off}
	$-\sqrt{2}F_0$	$-\sqrt{2}F_1$	$-2F_0$	0
$2^{-1/2}[\Omega_P^\dagger - \Omega_N^\dagger]$			E_i^{off}	$E_i = \epsilon_i + \delta\epsilon_i$
	$-aF_1$	aF_1	0	$-2F_1$

$=\langle T_0T_0|T^-=0$. Another interesting feature in Table I is the nondiagonal contribution from the single particle Hamiltonian arising between the states generated via operators (8a) and (8b).

D. RPA ground state

The ground-state RPA wave function[4,6] in terms of the new basis can be written as

$$|\Psi\rangle=N_0\exp\left\{-\tfrac{1}{2}\sum_{JM}\sum_{ij}\left[C^J_{ij}+\frac{B^J_{ij}}{E_i+E_j}\right](-)^{J-M}\Gamma^\dagger_{T_0T_0}(i,JM)\Gamma^\dagger_{T_0T_0}(j,J-M)\right\}|T_0T_0\rangle, \tag{23}$$

where the correlation matrix C^J is given by

$$Y^J=C^JX^J \tag{24}$$

and the energies E_i and matrix elements B^J_{ij} are specified in Table I.

The correlated ground state (23) is a direct generalization of the corresponding result obtained in Ref. 4 by explicit summation of the perturbation theory diagrams. Ellis[4] treats the particle-hole creation operators $A^\dagger$ [e.g., our Eq. (8)] as bosons and introduces the exchange correction term separately. Our $\Gamma^\dagger$ operators may be treated in precisely the same way since the additional $b^\dagger aT^-$ term, by the same argument as used in connection with (22), contributes only the usual 1p-1h expressions in the calculation of the correlation energy, normalization factor N_0, and occupation probabilities for the ground state (23).

The quasiboson form of the ground state, which corresponds to the omission of the second term in the square brackets of Eq. (23), can indeed be obtained in the formalism with projection operators P_{TT_z} by the direct application of the Sanderson[3] method.

III. SPECTROSCOPY OF ^{40}Ca AND ^{48}Ca

A. Residual interaction and the single-particle energies

The nonlocal separable Tabakin potential with $^1P_1$ phase parameters as in Ref. 15 has been used for calculating the matrix elements between p-h states. For the evaluation of the second-order Born corrections, the method of Clement and Baranger[15] was used. The parameters are as follows: Fermi momentum $K_F=1.3$ fm^{-1}, $W_0=-10.0$ MeV, harmonic-oscillator well parameter $b=2.063$ fm. The integration over c.m. momentum is from 0 to ∞.

Since several sets of single-particle and -hole energies have been introduced in the literature, we examined the stability of our numerical results against a change of these parameters. They are listed in Table II for the ^{40}Ca and ^{48}Ca nuclei. No Coulomb corrections are included in the case of ^{40}Ca.

Inclusion of the $0g_{9/2}$ single-particle (s.p.) state into the model space, though irrelevant in ^{40}Ca, would be desirable in the case of the ^{48}Ca nucleus

TABLE II. Single-particle energies ϵ_a (in MeV) of ^{40}Ca (rows 1–8) and ^{48}Ca (rows 9–12).

$\{\epsilon\}$ \ nlj	$1d_{5/2}$	$2s_{1/2}$	$1d_{3/2}$	$1f_{7/2}$	$2p_{3/2}$	$1f_{5/2}$	$2p_{1/2}$
			^{40}Ca				
DM (Ref. 18)	−13.10	−9.60	−7.10	0.0	1.70	5.95	3.25
ETh (Ref. 16)	−14.10	−9.10	−7.50	0.0	3.60	6.20	5.40
EEx (Ref. 16)	−13.50	−9.80	−7.20	0.0	2.10	5.50	4.10
D (Ref. 19)	−13.30	−9.80	−7.30	0.0	2.00	6.20	4.10
GP (Ref. 17)	−12.61	−9.51	−6.71	0.0	1.90	6.40	4.10
GN (Ref. 17)	−13.27	−10.17	−7.37	0.0	1.95	6.40	3.95
GAv (Ref. 17)	−12.94	−9.84	−7.04	0.0	1.95	6.40	3.95
Z (Ref. 20)	−11.70	−9.70	−7.20	0.0	1.90	6.25	4.25
			^{48}Ca				
JR (Ref. 12) neutron	−16.57	−13.63	−13.64	−9.94	−5.14	−1.18	−3.12
proton	−19.41	−15.26	−15.63	−9.62	−5.20	−3.67	−2.76
E (Ref. 16) neutron	−22.1	−13.5	−13.6	−7.6	−2.8	−1.0	−0.9
proton	−21.8	−15.5	−15.5	−9.5	−3.2	−2.7	−0.9

since there it opens many new excitation possibilities. Unfortunately, its position is not well established. Therefore we are forced to omit this state.

Since our final aim is to study the relative change of the rms radii from ^{40}Ca to ^{48}Ca we are especially interested in the pairs of the s.p. energy sets for these nuclei constructed by a unique prescription. The sets consistent in this sense are E and ETh calculated in Woods-Saxon potential well by Elton[16] and the pair GAv-JR extracted from the experimental separation energies of the neighboring nuclei by Gillet and Sanderson[17] and Jaffrin and Ripka.[12]

B. RPA results for ^{40}Ca

To be able to draw conclusions on the behavior of the nuclear radii we have to describe within the same scheme both the ^{40}Ca and ^{48}Ca nuclei. We used the symmetrized version of the RPA method[6] when calculating the ground and excited states of ^{40}Ca. The lowest $J^\pi = 1^-$, $T = 0$ state, which in the RPA calculations yields imaginary energy, is considered to be mostly spurious and has been excluded from further calculations. The lowest nonspurious solution is then related with the observed 1^- state at 6.94 MeV since the 1^- level at 5.90 MeV seems to belong to a rotational band. The resulting negative-parity excitation energies ω given in Table III are all about 1 MeV too high when compared with the experiment. In Table III we also list the probability P_0 of finding a double closed shell configuration in the ground state. P_2 and P_4 are probabilities to find two and four particles excited in the ground state.

The nice feature of these results is that they depend only slightly on the choice of the s.p. energies. Among many s.p. sets we have tried, the most extreme results were obtained with the ETh[16] single-particle scheme.

TABLE III. Eigenvalues ω (in MeV) for the various J^π, $T=0$ states compared with the experimental values for ^{40}Ca. The last three rows contain the probabilities P_{2n} for finding $2n$ particles excited in the RPA g.s. of ^{40}Ca.

J^π \ $\{\epsilon\}$	DM	ETh	D	GAv	Exp. [a]
1^-	7.82	10.15	8.54	8.17	6.94
3^-	4.26	4.78	4.67	4.46	3.73
	7.83	8.31	8.19	7.93	6.29
	8.63	10.28	8.96	8.81	6.58
5^-	5.63	6.10	5.85	5.57	4.48
P_0	0.399	0.482	0.449	0.406	
P_2	0.363	0.346	0.354	0.366	
P_4	0.154	0.119	0.133	0.165	

[a] See Ref. 21.

C. RPA results for ^{48}Ca

The energies of the negative- and positive-parity excited states of ^{48}Ca as obtained with the s.p. energy sets of Refs. 12 and 16 (see Table II) are compared with the experimental results in Table IV. Again the lowest 1^- state was omitted as highly spurious. The most interesting collective 3^- level is very satisfactorily described with the s.p. energy set JR[12]. Two groups of the observed J^- excited states centered at about 5.5 MeV (four states) and 7 MeV (five states) exhibit different behavior, e.g., the second group accounts for ≈75% of the β-decay strength of the ^{48}K nucleus.[22] These two groups are well separated in our calculation and they come out with correct spins and parities. Both groups are, however, shifted to higher energies by slightly less than 1 MeV (the Set JR) and by almost 3 MeV with the Set E. Despite the limitations of the chosen model space which is rather inappropriate for description of the positive-parity states (see Sec. III A) even the 2^+, 3^+, and 4^+ levels were obtained at an approximately correct position and with correct densities.

The decomposition of the RPA ground-state wave function of ^{48}Ca is displayed in Table V. The probabilities $P_{2k}(n)$ $[P_{2k}(p)]$ are those of the excitation of $2k$ neutrons (protons) in the ground state. (In our previous work the proton and neutron occupation probabilities should be 69 and 80%, respectively (p. 1246 of Ref. 6), they were interchanged in typing by mistake). Comparison of the

TABLE IV. Eigenvalues ω (in MeV) for the various J^π states compared with the experimental values for ^{48}Ca.

J^π \ $\{\epsilon\}$	JR	E	Exp. [a]
1^-	7.76	9.95	6.61
	7.98	10.85	7.30
2^-	7.10	7.26	6.69
	8.40	10.70	6.90
3^-	4.31	5.09	4.51
	6.27	6.38	5.37
	7.81	10.07	7.40
4^-	6.03	6.21	5.15
	6.48	6.68	5.25
5^-	5.99	6.09	5.73
2^+	4.85	4.85	3.83 [b]
3^+	5.03	5.02	4.61 [a]
4^+	4.84	4.84	5.15 [b]
	7.05	6.90	6.34 [b]

[a] See Ref. 22.
[b] See Ref. 21.

TABLE V. Probabilities P_{2k} for finding $2k$ neutrons (protons) excited above the Fermi level in the RPA ground state of ^{48}Ca. In the last column the average number $\bar{N}$ of excited particles above the Fermi level is given.

$\{\epsilon\}$	P_0	$P_0(n)$	$P_0(p)$	$P_2(n)$	$P_2(p)$	$P_4(n)$	$P_4(p)$	$\bar{N}$ neutron	$\bar{N}$ proton
JR	0.698	0.904	0.770	0.091	0.199	0.005	0.026	0.202	0.516
E	0.802	0.936	0.857	0.061	0.129	0.002	0.010	0.133	0.309

probability $P_0 = P_0(n) \times P_0(p) = 0.69$ to find the closed shells with the corresponding numbers for ^{40}Ca (Table III) shows that ^{48}Ca contains less correlations in the ground state. It can obviously be connected with the observation that the excited states of ^{48}Ca are, in general, higher than the corresponding ones in ^{40}Ca.

D. Radii and densities

Precision measurements performed recently with the high-energy electrons[8] and protons[23] provided detailed information on the root-mean-square (rms) radii of the charge, neutron, and matter distributions in atomic nuclei. In $N=Z$ ($A \geq 12$) nuclei the $r_{ch} \sim A^{1/3}$ rule is now well established. A less rapid growth ($\sim A^{1/5}$) was observed in the various chains of isotopes. In the Ca isotopes, on the other hand, the rms charge radius stays virtually constant from ^{40}Ca to ^{48}Ca: precise experiments[8] give even a small decrease with the result

$$\langle r^2 \rangle_{ch40}{}^{1/2} - \langle r^2 \rangle_{ch48}{}^{1/2} = +0.01 \text{ fm}.$$

To understand the origin of the anomaly, several calculations have been performed. Elton[24] built up the charge distribution from single-particle proton wave functions calculated in a spherical potential so as to fit s.p. separation energies and the electron scattering data. In such a fit acceptable agreement with the measured isotope shift was obtained. Hartree-Fock calculations with density-dependent residual interactions[25,26] and with the Tabakin and Hamada-Johnston potentials[27] result in isotope shifts of incorrect size and/or sign. Dramatic effects from neutrons caused by their charge form factor and spin-orbit interaction were found by Bertozzi *et al.*[28]: $f_{7/2}$ neutrons cause a decrease of the rms charge radius from ^{40}Ca to ^{48}Ca by 0.021 fm.

In the present investigation we study the role of the ground-state correlations in description of the rms radii and density distributions. The relative importance of the corresponding corrections can be seen from a comparison of the rms proton radius of the ^{48}Ca nucleus calculated with three different wave functions (w.f.). Starting with an uncorrelated ground state (harmonic oscillator) we obtain increase of 0.01 and 0.04 fm in the rms proton radius $\langle r^2 \rangle_p{}^{1/2}$ using the RPA g.s. w.f. of Ref. 6 and the sharp-isospin RPA g.s. w.f. constructed in Sec. II, respectively. Such large changes indeed deserve careful consideration.

From the calculation we get the rms radii corresponding to the distribution of the proton (neutron) centers. They are then corrected for the finite nucleon size ($\langle r_p{}^2 \rangle = \langle r_n{}^2 \rangle = 0.64$ fm^2); therefore our rms proton radius

$$\langle r^2 \rangle_p{}^{1/2} = (\langle r^2 \rangle_{cp} + \langle r_p{}^2 \rangle)^{1/2}$$

has to be compared with the observed radius of the charge distribution.

In what follows we present the results obtained with the RPA g.s. w.f. as given by Eq. (23). Let us stress once again that the processes responsible for the g.s. correlations are correctly summed up in Eq. (23) avoiding the earlier[2,3] "double counting" errors, and the correct value of the g.s. isospin quantum number in both ^{40}Ca and ^{48}Ca nuclei is guaranteed.

The free parameter of our method is the spring constant of the harmonic-oscillator basis functions. This parameter is of a "mathematical" origin and does not appear in the self-consistent (Hartree-Fock or Brueckner-type) theories. In the shell-model calculations ν is traditionally fixed separately for each nucleus. Since we are looking just for the behavior of the nuclear radii which is mostly affected by the parameter ν, it would be particularly unsatisfactory to introduce two different values of ν for ^{40}Ca and ^{48}Ca. We assume that $\nu_{40} = \nu_{48} = \nu$ and argue that if the incorporation of the ground-state correlations is to be considered as a valid explanation of the isotope effect it must provide an answer independent of ν. Actually we have calculated the differences $d = \langle r^2 \rangle_{p40}{}^{1/2} - \langle r^2 \rangle_{p48}{}^{1/2}$ and $\Delta = \langle r^2 \rangle_{n48}{}^{1/2} - \langle r^2 \rangle_{p48}{}^{1/2}$ over a broad range of the harmonic-oscillator (h.o.) constant $0.23 \text{ fm}^{-2} \leq \nu \leq 0.30 \text{ fm}^{-2}$ with the results stable within 5% over this range for both d and Δ.

Further, we were interested in whether the single-particle energies which go as input values into the RPA part of the calculation do appreciably

TABLE VI. The rms proton radius of ^{40}Ca (in fm), columns are labeled by the s.p. energy sets introduced in Table II. We have $\langle r^2\rangle_p^{1/2} = \langle r^2\rangle_n^{1/2} = \langle r^2\rangle_m^{1/2}$. The measured values are 3.4869 fm (250 MeV electrons), 3.526 fm (500 MeV electrons), and 3.491 fm (1 GeV protons) obtained by Frosch *et al.* (Ref. 8) and Alkhazov *et al.* (Ref. 23), respectively. To show that the results do not change appreciably with the shifts of s.p. energies we fixed deliberately the h.o. constant, $\nu = 0.265$ fm^{-2}.

$\{\epsilon\}$	DW	ETh	EEx	D
$\langle r^2\rangle_{ch40}^{1/2}$	3.4855	3.4790	3.4834	3.4818
$\{\epsilon\}$	GP	GN	GAv	Z
$\langle r^2\rangle_{ch40}^{1/2}$	3.4903	3.4824	3.4857	3.4882

influence our results. The calculated values of the proton rms radius of ^{40}Ca obtained with eight different single-particle energy sets of Table II are given in Table VI. As a matter of fact, the results are more stable against the changes in s.p. energy sets than expected. Relying on the above argument we have deliberately chosen $\nu = 0.265$ fm^{-2}; therefore comparison with the observed values is useless. Similarly the rms radii of the proton, neutron, and matter distributions in ^{48}Ca as given in Table VII are intended to demonstrate their relative independence on the s.p. energy sets. The measured quantities are only displayed for the reader's convenience.

After this preliminary discussion of the stability of our calculation against the free parameters we shall present the most interesting quantities which characterize the isotope shift and the difference of the proton and neutron distributions in ^{48}Ca. The relative change of the charge rms radius $R = (\langle r^2\rangle_{ch48}^{1/2} - \langle r^2\rangle_{ch40}^{1/2})/\langle r^2\rangle_{ch40}^{1/2}$ was precisely measured in 250 and 500 MeV electron scattering experiments by Frosch.[8] Our calculated results which are given in Table VIII were obtained with the s.p. energy sets GAv-JR and ETh-E of Table II. As discussed in Sec. II these sets should be most appropriate for calculation of such relative quantities. Let us note, however, that for all other pairs of s.p. energy sets the results are remarkably stable varying from -0.17 to -0.49% as compared with the order-of-magnitude larger positive and negative values calculated by other authors, which are also displayed in Table VIII. Our calculations are in close agreement with the measured value $R = -0.31\%$ as obtained by Frosch *et al.*[8]

The calculated and experimental results for the difference $\Delta = \langle r^2\rangle_{n48}^{1/2} - \langle r^2\rangle_{p48}^{1/2}$ of the neutron and proton rms radii are given in Table IX. Consistent with the previous theoretical investigations and with early experiments we found that the neutron distribution extends beyond the proton distribution in ^{48}Ca. Recently, scattering of 79 MeV α particles[35] led to the value $\Delta = 0.03 \pm 0.08$ fm. The reason for this discrepancy may lie in some fine details of the optical-model analysis which necessarily introduces certain simplifications. On the other side, the Glauber model used in the analysis of the 1 GeV data[34] is currently considered most reliable and the results obtained both at the Leningrad[34] and Saclay[34] machine nicely agree with our calculation.

It is well known that neither single-particle models[16] nor Hartree-Fock calculations[27] (with den-

TABLE VII. The rms radii $\langle r^2\rangle_p^{1/2}$, $\langle r^2\rangle_n^{1/2}$, and $\langle r^2\rangle_m^{1/2}$ of the proton, neutron, and matter distributions in ^{48}Ca (in fm). The first and second row contain our calculated results labeled by the input s.p. energy sets defined in Table II. The other are experimental results. Again the h.o. constant is deliberately fixed at $\nu = 0.265$ fm^{-2}.

Method	Reference	$\langle r^2\rangle_{p48}^{1/2}$	$\langle r^2\rangle_{n48}^{1/2}$	$\langle r^2\rangle_{m48}^{1/2}$
$\{\epsilon\}$ = JR	This paper	3.4733	3.6883	3.6002
$\{\epsilon\}$ = E	This paper	3.4669	3.6863	3.5965
e^- (250 MeV)	8	3.4762	···	···
e^- (500 MeV)	8	3.5170	···	···
p (1 GeV) [a]	34 [b]	3.443	3.661	3.572
p (1.044 GeV) [a]	34 [c]	3.443	3.645	3.562
p (1 GeV) [d]	34 [b]	3.513	3.633	3.584
p (1.044 GeV) [d]	34 [c]	3.513	3.621	3.576
p (1.044 GeV) [e]	.34 [c]	3.475	3.661	3.585

[a] Charge parameters for $E_\beta = 250$ MeV taken from Ref. 8 were used in data analysis.
[b] Leningrad results.
[c] Saclay results (Saturn I).
[d] Charge parameters for $E_\beta = 500$ MeV taken from Ref. 8 were used in data analysis.
[e] Charge parameters taken from Ref. 8 ("main result") were used in data analysis.

TABLE VIII. The ratio $R=[\langle r^2\rangle_{p48}^{1/2}-\langle r^2\rangle_{p40}^{1/2}]/\langle r^2\rangle_{p40}^{1/2}$ (in %) calculated in the present work and by other authors. The electron scattering measurement by Frosch *et al.* (Ref. 8) yields $R_{\rm exp}=-0.31\%$.

Present work		R	Ref.
R	$\{\epsilon\}$	−0.593	Elton (Ref. 24)
−0.355	GAv-Jr	+1.111	Negele (Ref. 25)
−0.348	ETh-E	+1.436	Vautherin *et al.* (Ref. 26)
		−3.690	Lande et al. (Ref. 22)
		+4.444	Meldner (Ref. 29)

sity-independent nuclear interactions) are able to reproduce the detailed density distributions. As demonstrated above, the ground-state correlation effects proved to be important for the correct description of the nuclear radii. Therefore it was interesting to study the question of whether our RPA method is also capable of producing the density distributions in agreement with experiment.

It was known from the time of the first high momentum transfer ($q>3$ fm^{-1}) electron scattering experiments[36] that the nuclear charge densities differ from the early assumed structureless distributions by a distinct peak of $\rho(r)$ at $r=0$. Recent analysis of the available high momentum transfer measurements together with the x-ray data[37] discovered even a discrete ambiguity of $\rho(r)$ at small radii, the solution with the higher central peak being better founded in the case of ^{40}Ca. Such a feature can be qualitatively understood in terms of the shell model; it is connected with the pronounced narrow peak of the $1s_{1/2}$ single-particle wave function. Quantitatively, however, the earlier theoretical attempts predicted this peak by a factor of about 2 too high. It has been shown by Negele[25] that the dependence of the nuclear potential on local density (plus suitable modification of the HF theory) contributes strongly to depressing the central density (see Fig. 4 of Ref. 25). Comparison of Negele's and our results for ^{40}Ca in Fig. 1 shows that the ground-state correlations introduced by RPA produce a similar flattening of the distribution. In the most interesting case of ^{48}Ca we also found considerable improvement of the theoretical $\rho(r)$ due to the incorporation of g.s. correlations as can be seen from Fig. 2.

The calculated density distributions have to be corrected for the center-of-mass motion effects and for the finite proton size. These corrections were calculated in the standard manner (see, e.g., Ref. 25) for the ^{40}Ca proton distribution. Further flattening of $\rho(r)$ near the origin appears. In concluding we must emphasize that in spite of sizable effects from the g.s. correlations the calculated density distributions still differ from those extracted from experiments, especially the region of small radii is poorly known.

The difference in the charge density distributions $4\pi r^2(\rho_{40}-\rho_{48})$ is believed to be the most precisely measured isotope effect.[8] Bearing in mind the above mentioned deficiencies in description of the individual densities ρ_{40} and ρ_{48} we can hardly expect good results when calculating their difference. Actually we have tried all combinations of the s.p. energy sets of Table II and several values of the harmonic oscillator constant ν. The results differ strongly from each other while retaining, however, two common features: (i)

TABLE IX. The difference in rms radii of the neutron and proton distributions $\Delta=\langle r^2\rangle_{n48}^{1/2}-\langle r^2\rangle_{p48}^{1/2}$ (in fm) for the ^{48}Ca nucleus calculated in the present work (rows 1 and 2) is compared with other theoretical and experimental results.

$\Delta_{\rm theor}$	Reference	$\Delta_{\rm exp}$	Method	Reference
0.215	$\{\epsilon\}$ = JR	0.13 [a]	p (1 GeV)	Alkhazov (Ref. 23)
0.219	$\{\epsilon\}$ = E	0.22 [b]	p (1 GeV)	Alkhazov (Ref. 34)
0.34	Elton (Ref. 24)	0.39	p (11–16 MeV)	Lombardi (Ref. 30)
0.23	Negele (Ref. 25)	0.21 [c]	α (42 MeV)	Fernandez (Ref. 31)
0.12	Vautherin (Ref. 26)	0.20 [c]	α ($\approx$30 MeV)	Bernstein (Ref. 32)
0.27	Lande (Ref. 27)	0.17 [c]	p (25–40 MeV)	Maggiore (Ref. 33)
0.14	Meldner (Ref. 29)	0.03 ± 0.08	α (79 MeV)	Lerner (Ref. 35)

[a] Corrections for the neutron form factor and spin-orbit interaction (Ref. 28) included.
[b] See also Table VII.
[c] Values calculated by Lombardi *et al.* (Ref. 30) from the data of Refs. 31–33.

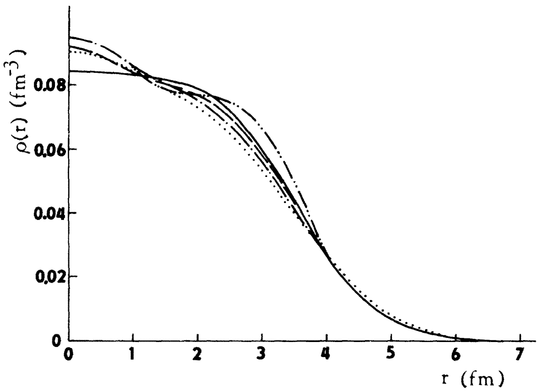

FIG. 1. Density distributions for protons in ^{40}Ca [for RPA (dot-dash line)] and [for RPA with center-of-mass and finite proton size corrections (dotted line)] are compared with results by Negele (dot dot-dash line, Ref. 25, Fig. 5) and with experimental distributions (full line, Ref. 8 and dash-line, Ref. 34).

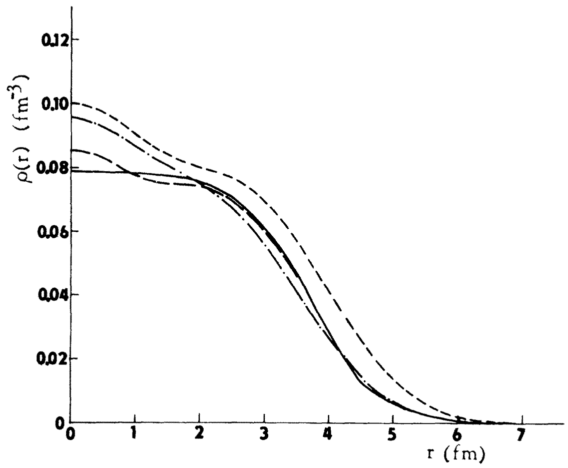

FIG. 2. Density distributions in ^{48}Ca for protons (dot-dash line) and for neutrons (short-dash line) from present work (no c.m. or proton size corrections) are shown together with the experimental charge distributions (full line, Ref. 8 and long-dash line, Ref. 34).

Near the origin the difference $\rho_{40} - \rho_{48}$ is negative in contrast with the experiment; and (ii) both minimum and maximum of the difference are too large in absolute value. We conclude that just as in the previous theoretical approaches, we are unable to describe this fine effect.[38]

IV. CONCLUSION

The RPA ground-state wave function for the $N \neq Z$ doubly magic nuclei has been constructed. The sharp value of the isospin quantum number $T_0 = (N - Z)/2$ is ensured by applying the appropriate projection. As an example we have analyzed the ^{48}Ca nucleus. The spectrum of the low-lying excited states was obtained as a byproduct when constructing the g.s. wave function. The spectrum (especially the important collective states) is in fair agreement with the experiment.

Our main aim was to explain the isotope "anomaly" observed for the charge radii in calcium isotopes: the measured rms charge radius decreases from ^{40}Ca to ^{48}Ca by 0.01 fm. In our RPA approach we were able to show that the ground-state correlations provide an appropriate explanation of the effect if introduced with care of the isospin conservation. The parameter-independent numerical result was obtained for the difference of rms proton radii in ^{40}Ca and ^{48}Ca, in excellent agreement with the high energy electron scattering experiment by Frosch *et al.*[8] Similarly we reproduce very well the difference of the neutron and proton rms radii in ^{48}Ca as recently measured at two high energy proton accelerators.[34] An important improvement was also obtained for the density distributions. Further work is, however, necessary both on theoretical and experimental side (larger q values with better statistics) in order to draw definite conclusions about the central densities. Our results show that the ground-state correlation effects are numerically at least as important as several others already discussed in the theory of nuclear radii (e.g., neutron form factor and spin-orbit interaction, Ref. 28) and most probably should be considered on the same footing.

We express our thanks to Professor G. D. Alkhazov for the correspondence concerning the 1 GeV proton experiments.

[1]G. E. Brown, *Unified Theory of Nuclear Models and Nuclear Forces* (North-Holland, Amsterdam, 1967).

[2]G. E. Brown and G. Jacob, Nucl. Phys. 42, 177 (1963).

[3]E. A. Sanderson, Phys. Lett. 19, 141 (1965); D. Agassi, V. Gillet, and A. Lumbroso, Nucl. Phys. A130, 129 (1969).

[4]D. J. Rowe, Phys. Rev. 175, 1283 (1968); R. E. Johnson, R. M. Dreizler, and A. Klein, Phys. Rev. 186, 1289 (1969); P. J. Ellis and L. Zamick, Ann. of Phys. (N.Y.) 55, 61 (1969); J. da Providência and J. Weneser, Phys. Rev. C 1, 825 (1970); P. J. Ellis, Nucl. Phys. A155, 625 (1970).

[5]See, e.g., *Isospin in Nuclear Physics*, edited by D. H. Wilkinson (North-Holland, Amsterdam, 1969). C. A. Engelbrecht and R. H. Lemmer, Phys. Rev. Lett. 24, 607 (1970); H. C. Lee, *ibid.* 27, 200 (1971).

[6]E. Gmitrová, M. Gmitro, and Y. K. Gambhir, Phys. Rev. C 4, 1239 (1971).
[7]J. K. Parikh, Phys. Rev. C 8, 1433 (1973).
[8]R. F. Frosch *et al.*, Phys. Rev. 174, 1380 (1968).
[9]M. Soga, Nucl. Phys. A143, 652 (1970).
[10]P. O. Löwdin, Rev. Mod. Phys. 36, 966 (1964).
[11]D. J. Rowe, J. Math. Phys. 10, 1774 (1969).
[12]A. Jaffrin and G. Ripka, Nucl. Phys. A119, 529 (1968).
[13]D. J. Rowe, Rev. Mod. Phys. 40, 153 (1968).
[14]D. J. Rowe and C. Ngo Trong, Rev. Mod. Phys. 47, 471 (1975).
[15]D. M. Clement and E. U. Baranger, Nucl. Phys. A108, 27 (1968).
[16]L. R. B. Elton and A. Swift, Nucl. Phys. A94, 52 (1967).
[17]V. Gillet and E. A. Sanderson, Nucl. Phys. 54, 472 (1964).
[18]M. Dworzecka and H. McManus, Phys. Lett. 37B, 331 (1971).
[19]A. E. L. Dieperink, H. P. Leenhouts, and P. J. Brussaard, Nucl. Phys. A116, 556 (1968).
[20]P. Goode and L. Zamick, Nucl. Phys. A129, 81 (1969).
[21]E. P. Lippincot and A. M. Bernstein, Phys. Rev. 163, 1170 (1967).
[22]L. G. Multhauf, K. G. Tirsell, S. Raman, and J. B. McGrory, Phys. Lett. 57B, 44 (1975).
[23]G. D. Alkhazov *et al.*, Phys. Lett. 57B, 47 (1975).
[24]L. R. B. Elton, Phys. Rev. 158, 970 (1967).
[25]J. Negele, Phys. Rev. C 1, 1296 (1970).
[26]D. Vautherin and D. M. Brink, Phys. Lett. 32B, 149 (1970).
[27]A. Landé and J. Svenne, Nucl. Phys. A164, 49 (1971).
[28]W. Bertozzi, J. Friar, J. Heisenberg, and J. W. Negele, Phys. Lett. 41B, 408 (1972).
[29]H. Meldner, Phys. Rev. 179, 1815 (1969).
[30]J. C. Lombardi, R. N. Boyd, R. Arking, and A. B. Robbins, Nucl. Phys. A188, 103 (1972).
[31]B. Fernandez and J. S. Blair, Phys. Rev. C 1, 523 (1970).
[32]A. M. Bernstein, M. Duffy, and E. P. Lippincot, Phys. Lett. 30B, 20 (1969).
[33]C. J. Maggiore, C. R. Gruhn, T. Y. T. Kuo, and B. M. Preedom, Phys. Lett. 33B, 571 (1970).
[34]G. D. Alkhazov *et al.*, Leningrad Nuclear Physics Institute, Report No. 218, 1976 (unpublished).
[35]G. M. Lerner, J. C. Hiebert, L. L. Rutledge, Jr., C. Papanicolas, and A. M. Bernstein, Phys. Rev. C 12, 778 (1975).
[36]J. B. Bellicard *et al.*, Phys. Rev. Lett. 19, 527 (1967).
[37]I. Sick, Phys. Lett. 53B, 15 (1974).
[38]Relativistic calculation by L. D. Miller and A. E. S. Green, Phys. Rev. C 5, 241 (1972) is likely the only exception. They reproduce very well the experimental $4\pi r^2(\rho_{40}-\rho_{48})$ curve.